A Numerical Case Study on the Sensitivity of the Water and Energy Fluxes to the Heterogeneity of the Distribution of Land Use

Katja Friedrich and Nicole Mölders

Summary:

Numerical experiments assuming land-use distributions of different heterogeneity of wet and dry surfaces were performed on a cloudy day in spring with a calm wind to examine their influences on the domain-averaged fluxes as well as on the distribution of the fluxes within the domain. The results substantiate that, for large heterogeneity, i.e., small patches, the distribution of the patches plays no role in the magnitude of the atmospheric fluxes. For larger patches, however, the domain-averaged latent heat-fluxes depend appreciably on both the heterogeneity as well as on the fractional coverage by the land-use types. On the average, for heterogeneous conditions, the prevailing land-use type governs the fluxes. Nevertheless, no exact linearity between the fractionally coverage of the two land-use types and the resulting fluxes exists. Discontinuities in the fluxes which lead to the non-linear behaviour of the domain-averaged fluxes occur at the border between two larger areas of extremely different characteristics, namely, *grass* (wet, cool) and *sand* (dry, warm). Three different patterns of behaviour are found for the temporal development of the differences in the domain-averaged fluxes which depend on both the heterogeneity and the pattern of the land use.

Zusammenfassung:

Numerische Experimente, bei denen unterschiedlich heterogene Landnutzungsverteilungen trockener und feuchte Flächen angenommen werden, wurden für einen wolkigen Schwachwindtag im Frühjahr durchgeführt. Die Ergebnisse belegen, daß bei großer Heterogenität, d.h. kleinen Flächen, deren Anordnung keine Rolle spielt. Bei großen Flächen jedoch hängen die Gebietsmittelwerte der latenten Wärmeflüsse merklich sowohl von der Heterogenität als auch von dem Flächenanteil der Landnutzung ab. Im Mittel beherrscht der vorherrschende Landnutzungstyp die Flüsse. Dennoch ist kein exaktes lineares Verhalten zwischen dem Flächenanteil der Landnutzung und den resultierenden Flüssen vorhanden. Diskontinuitäten in der Verteilung der Flüsse, die letztendlich zu der Nichtlinearität der Gebietsmittelwerte der Flüsse führen, treten an den Grenzen der größeren Flächen unterschiedlicher Oberflächencharakteristika auf, in dieser Studie Gras (feucht, kühl) und Sand (trocken, warm). Drei unterschiedliche Verhaltensweisen im zeitlichen Verlauf der Differenzen der Gebietsmittelwerte der Flüsse wurden gefunden, die vom Muster und der Heterogenität der Landnutzung abhängen.

1. Introduction

Flying over a landscape in mid-latitudes on a day with calm winds presents a fantastic view over patchy domains of various surfaces and sizes. Recently, observational, theoretical and numerical studies illustrated the impact of surface characteristics and discontinuities on the atmospheric boundary layer (ABL; e.g., Anthes 1984, Avissar and Pielke 1989, Mahrt et al. 1994). This impact is exacerbated by the moistening of the low-level atmosphere through transpiration, the rising of the resulting lighter, moist air (as compared to dry), and the additional ascending motion induced by surface thermal heterogeneity. The ascent and descent of air induced by surface heterogeneity tend to disappear, however, when surface wind speeds exceed 4 m/s due to turbulence (Shen and Leclerc 1994).

The horizontal grid resolution of meteorological models is much coarser than that required by hydrological studies. Moreover, a grid element of a meso-β-scale meteorological model encompasses several square kilometers for which often the dominant land-use type is assumed to be the representative one to determine the water and energy fluxes at the earth's surface. Since landscapes are often heterogeneous over the resolvable scales considered in meteorological models of that mesoscale, it has to be expected that the practice frequently applied to calculate the water and energy fluxes on the basis of dominant land-use types may be inadequate to represent the surface forcing because different land surfaces and slopes yield different fluxes of momentum, moisture, and heat (due to differences in water availability) as well as insulation, plant, and soil parameters (e.g., Avissar and Pielke 1989). Recently, several authors examined the behaviour of fluxes under heterogeneous surface conditions. Using different horizontal grid resolutions and assuming the dominant land-use type within a grid box as the representative surface type for the entire grid element, Mölders and Raabe (1996) showed that the grid resolution may strongly affect the calculated water and energy fluxes because a land-use type (being of subgrid-scale on a coarse grid and here of minor importance) may be dominant on a finer grid.

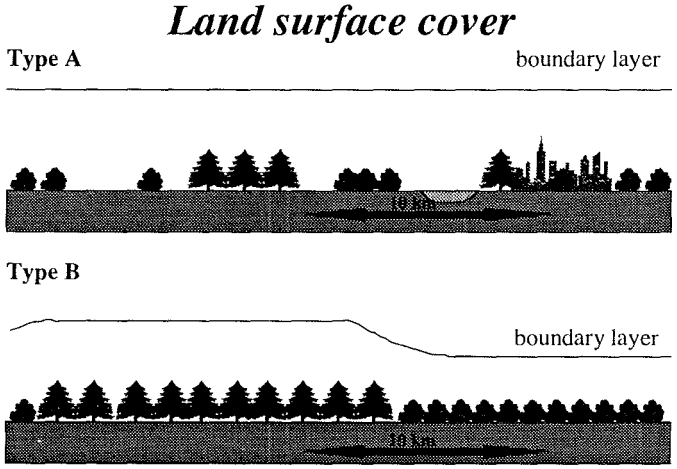

Fig. 1. Schematic view of the atmospheric response to the underlying surface for land-use type A and B (modified after Shuttleworth (1991)).

Recently, Shuttleworth (1988) proposed two distinct scales of land-cover influence: a 'disorganised' land surface (type A land-surface cover; Fig. 1), whose characteristic horizontal scales are less than 10 km, and an 'organised' land surface of characteristic length > 10 km (type B land-surface cover; Fig. 1). He theorised that only larger organised heterogeneity allows the atmosphere to develop a coherent response to land cover as substantiated by the formation of clouds and precipitation because the convective fluxes are aggregated over larger horizontal and vertical scales. It appears that there are two scales that need to be examined, i.e., the scale of about 100 km for homogeneous land-cover types, and the scale of 10 km or so, for heterogeneous land-cover types (O'Neal 1996). The emphasis of the present study is on investigating the role that the degree of heterogeneity of land use plays on the 'disorganised' modulation of the water and energy fluxes. In doing so, results provided by numerical simulations with different patterns of surface heterogeneity (Fig. 2) are compared and evaluated.

2. Model Description and Initialisation

The Leipzig version of the non-hydrostatic meteorological model GESIMA (Geesthacht's Simulation Model of the Atmosphere; Kapitza and Eppel 1992, Eppel et al. 1995) was used to investigate the response of the water and energy fluxes to the heterogeneity of the underlying

surface. Its dynamical part is based on the anelastic equations. The model's physical features are as follows: A five water-classes cloud-parameterisation scheme was applied (Mölders et al. 1997). The treatment of the soil/vegetation/atmosphere interaction follows Deardorff (1978, see also Eppel et al. 1995), assuming homogeneous soil and land-surface characteristics within a grid cell. The surface stress and the near-surface fluxes of heat and water vapour are expressed in terms of dimensionless drag and transfer coefficients applying the parametric model of Kramm et al. (1995). Radiation transfer is calculated by a simplified two-stream method (Eppel et al. 1995).

A homogeneous flat terrain was assumed for all simulations. The model was initiated using profiles of air temperature and humidity typical for a cloudy atmosphere in spring. A geostrophic wind of 8 m/s from the west was assumed. The simulations were integrated for 24 hours where the first six hours serve as the adjusting phase. The whole test domain has a size of 75 x 75 km^2 with a horizontal resolution of 5 x 5 km^2. The vertical resolution varies from 20 m close to the ground to 1.5 km at the top. The model whole domain has a hight of 10.5 km. Eight levels are located below the 2-km height and 7 are above.

3. Design of the Numerical Experiments

The investigations are performed for different patches of a *sand /grass* mixture which differ not only in the amount but also in the heterogeneity. Sixteen simulations with heterogeneous land-surface conditions are performed and two with homogeneous. In the two simulations assuming homogeneous surface conditions, the entire domain is covered by *grass* and *sand.* These runs will be addressed as HOMG and HOMS hereafter. Eight simulations assuming heterogeneous land-surface conditions are performed with altering *sand* and *grass* strips equal in width to 25 km and 5 km, respectively. The strips are once orientated in NS-direction perpendicular to the direction of the geostrophic wind and once in EW-direction parallel to the geostrophic wind (Fig. 2). These runs are referred to as GSGP25, SGSP25, GSGR25, SGSR25, GSGR5, SGSR5, GSGP5, SGSP5, where G stands for *grass*, and S for *sand*, respectively. The letters P and R represent the orientation of the strips to the wind direction, namely, *parallel* and *perpendicular.* Furthermore, six simulations are carried out using a chessboard for which the squares have a length of 25 km, 10 km and 5 km (Fig. 2). These runs are referred to as GSGC25, SGSC25, GSGC10, SGSC10 (where the last east and the last south row have a 10 x 15 km^2 resolution), GSGC5, GSGC5, where G and S represent the *grass* and *sand* land use as mentioned above, and C stands for *chessboard*, respectively. Two further simulations are performed with a north-south- and east-west-orientated cross which consists of five homogeneous 25 x 25 km^2 patches in the centre and four alternating 25 x 25 km^2 *sand* or *grass* patches on each corner (Fig. 2). These simulations are denoted as GSGX25 and SGSX25, respectively, where X stands for *cross*.

On summarising, the name of a simulation consists of six letters: the first three represent the land use (GSG, SGS) while the last three letters stand for the patch size and the patch arrangement (Fig. 2). In the following discussion we use xxx representing all variations of land use for a specific arrangement (xxxC25) or for all arrangements with a specific variation of land use (SGSxxx).

The dependency of the energy budget on the heterogeneity of the underlying surface is examined as follows. First, the temporal development of the domain averages of the components of the energy budget (fluxes of latent and sensible heat, soil heat-flux, net radiation) was determined for each simulation on an hourly basis for the entire simulation time (Fig. 4, sect.4.1.). In addition, we use this directly to compare the energy budget of simulations with the same amount of *grass* and *sand* but different heterogeneity (Fig. 5, sect. 4.2.).The differences of the domain averages of the 'homogeneous' to the 'heterogeneous' simulations are investigated by subtracting the domain averages of the respective heterogeneous simulations from those of HOMG and HOMS (Fig. 6, sect.4.3.).

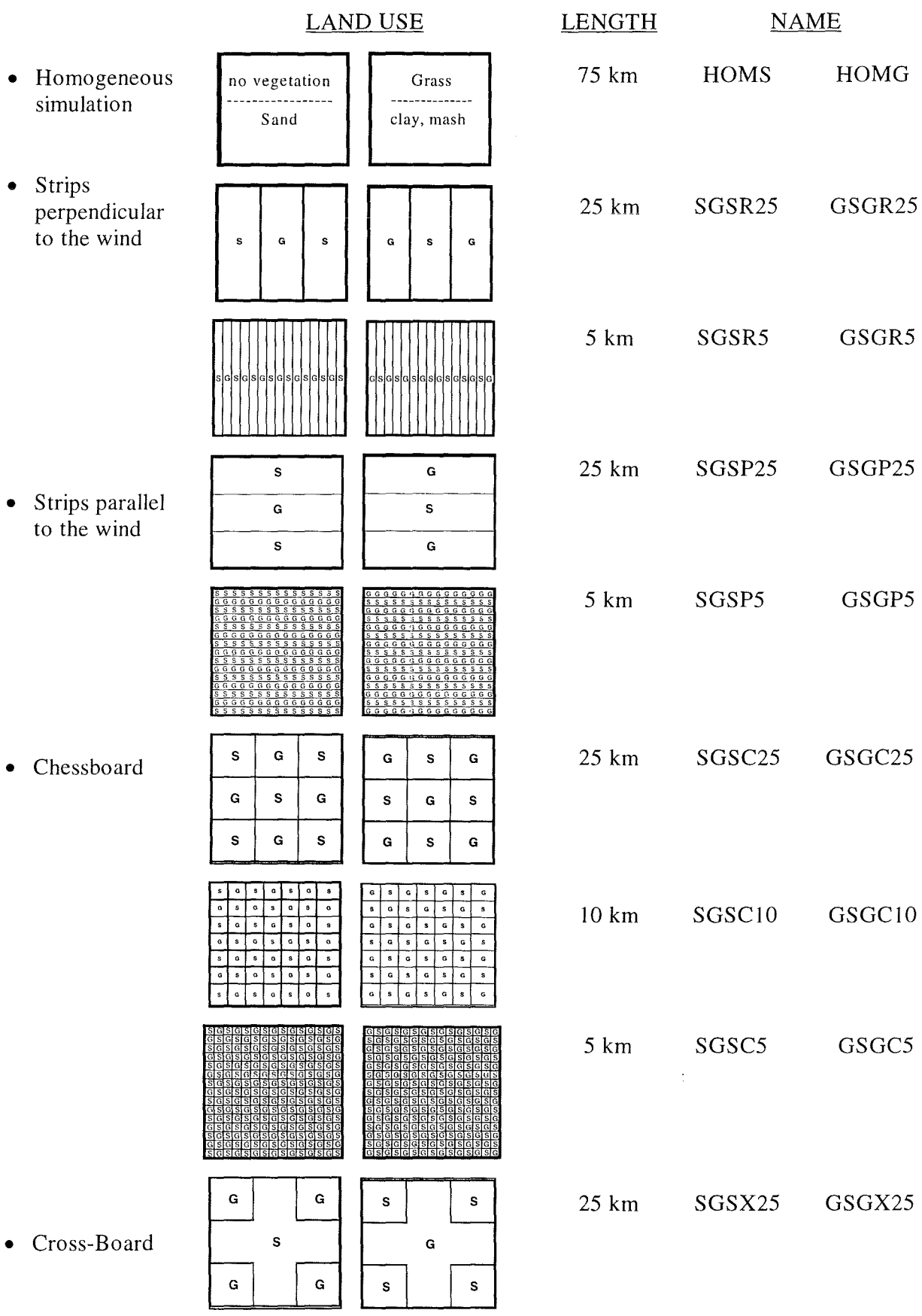

Fig. 2. Schematic view of the land-use distribution applied in the numerical experiments peformed for this study.

To investigate the contribution of a *grass*- and a *sand*-covered patches in the 'heterogeneous' simulations, the fractionally weighted domain averages of the homogeneous runs were subtracted from the domain averages of fluxes of the heterogeneous runs (Fig. 7, sec.4.4.). Herein, the area covered by the same land use in both runs determines the fractional weight (Eq. 1). For purposes of understanding factionally weighted land-use constribution we created the following equation:

$$F^K(HET) = \alpha F^K(HETi) + (1-\alpha) F^K(HETj) = \beta [\alpha F^K(HOMi) + (1-\alpha) F^K(HOMj)] \quad [1]$$
$$\text{with } i \neq j ,$$

where the index K stands for the fluxes of latent heat, Q_{lat}, sensible heat, Q_{sens}, soil heat, Q_{soil}, and net radiation, Q_{rad}, respectively. The idea behind this is as follows: If the contribution of the different patches add up linearly, then the differences (determined according to Eq. 1) will be the same as 1 minus the residuum of the fractional weight times the domain-averaged flux of the respective other homogeneous run. In the linear case, β would be equal to 1. By comparing these results, we can quantify the effect of the heterogeneity. Finally, a grid-point-by-grid-point comparison of the fluxes provided by the different simulations was performed to investigate where potential non-linear behaviour existed (Fig. 8).

The aim of these experimental designs is (1) to show the amount and the time of deviation (Figs. 6, 7) and (2) to investigate how the heterogeneous simulations average between the response to *grass* and *sand*, respectively (Fig. 8).

4. Results and Discussions

4.1. Impact of heterogeneity on energy budget

On the average, net radiation and the sensible heat-flux hardly differ for the different underlying surfaces. Generally, the increase of the soil heat-flux is at the expense of the sensible and latent heat-flux for a *grass*-dominated land surface, as compared to that obtained in the case of homogeneous coverage by *grass*. While for a *sand*-dominated land surface the soil heat-flux enhances by reducing the latent heat-flux. Therefore, in most parts of the article the latent heat- fluxes are discussed exemplarily.

By comparing each flux, similar results as illustrated in Fig. 3 are found. Although no great differences of fluxes will be expected at a latitude of 51° north, we found some differences in time of maximum of the fluxes and amount of fluxes (e.g., Figs. 2, 3, 4, Tabs. 4, 5). The more often *sand* occurs in the domain, the more the fluxes behave like *sand*. Therefore a maximum of *grass* and a minimum of *sand* occur for the sensible and latent heat- flux and a maximum of *grass* and a minimum of *sand* are found for the soil heat-flux and the net radiation.

If there were a linear response of the fluxes to the fractionally coverage by a certain land- use type, we should expect the magnitude of the domain-averaged fluxes to arrange themselves as given in Tab. 1.

NUMBER	NAME	AMOUNT OF *GRASS* IN 225TH
1	HOMG	225
2	GSGP25	150
3	GSGR25	150
4	GSGX25	125
5	GSGC25	125
6	GSGR5	120
7	GSGP5	120
8	GSGC10	117
9	GSGC5	113

NUMBER	NAME	AMOUNT OF *GRASS* IN 225TH
10	SGSC5	112
11	SGSC10	108
12	SGSR5	105
13	SGSP5	105
14	SGSC25	100
15	SGSX25	100
16	SGSP25	75
17	SGSR25	75
18	HOMS	0

Tab. 1. Arrangement of the simulations as expected for a linear response of the fluxes according to the fractionally coverage of *grass*.

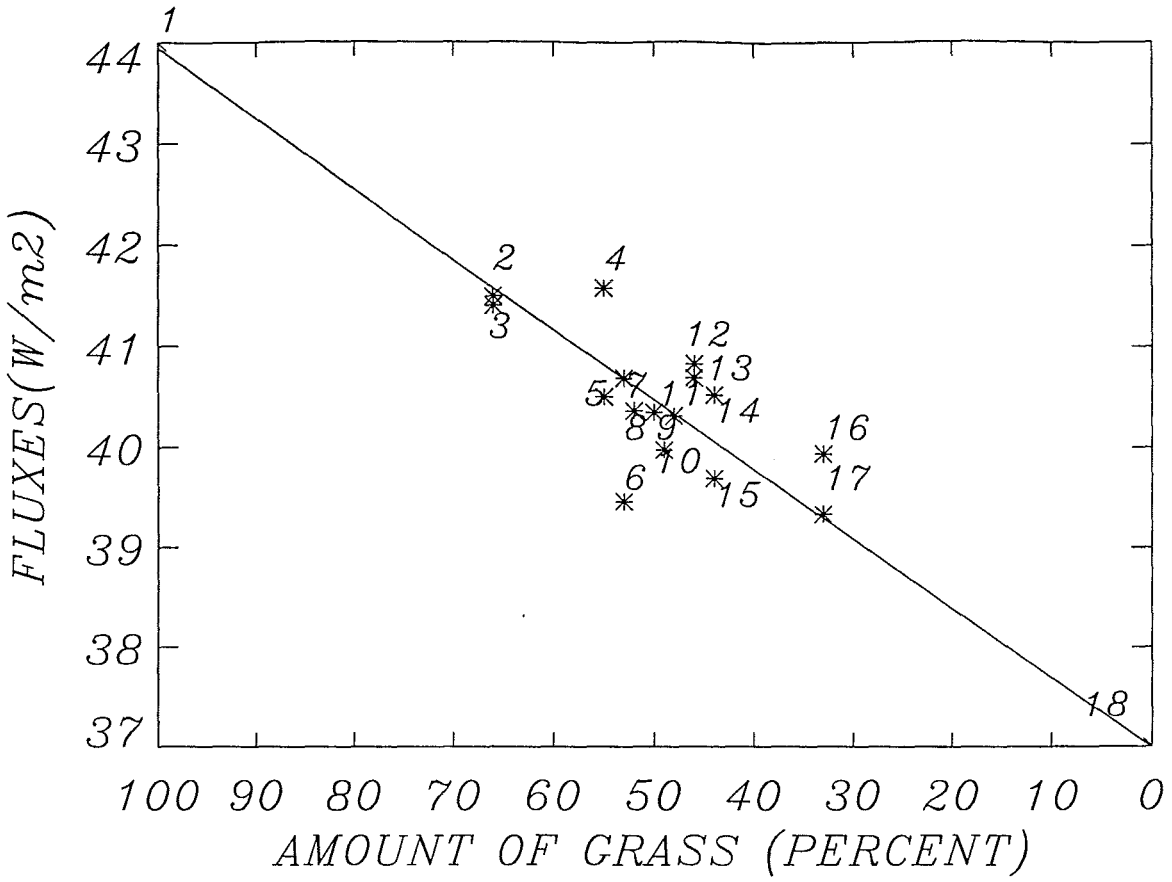

Fig. 3. Sensitivity of the domain averaged latent heat-fluxes for different fractional coverage of *grass* and *sand*, respectively, as well as for different patch arrangements at 1200LT. The numbers code the simulations as explained in Tab. 1.

The tendency of each simulation is exemplarily demonstrated in Fig. 3 for the flux of latent heat at 1200 LT. Obviously there are deviations from linearity, especially for fractional coverage around 50 %.

In the following chapter we compare all domain-averaged fluxes obtained for the different heterogeneous simulations to each other. For better comprehension of the correlation between increasing heterogeneity and the behaviour of the latent heat-flux, we use the following subjective way of arranging the simulations after heterogeneity (Tab. 2):

Ranging	Simulation name	Size of the largest patch
1	HOMx	75 x75 km (5625 km²)
2	xxxX25	5x25x25 km (3125 km²)
3	xxxP25	25x75 km (1875 km²)
4	xxxR25	25x75 km (1875 km²)
5	xxxC25	25x25 km (625 km²)
6	xxxP5	5x75 km (375 km²)
7	xxxR5	5x75 km (375 km²)
8	xxxC10	10x15 km (150 km²)
9	xxxC5	5x5 km (25 km²)

Tab. 2. Illustration of the heterogeneity according to the extension of the largest patch. Here it is assumed that the parallel strips have fewer effects on the energy budget than the perpendicular strips because the wind blows from the west and gets less affected by parallel strips than by perpendicular ones. The xxx stands for the subsequent combination of either SGS or GSG, and x represents *grass*, G, and *sand*, S.

Due to the different distributions of the surface energy budget of a mainly *grass*- or *sand*-covered surface (latent heat-flux for *grass* is larger than for *sand*), we divided the comparison of energy budget in *grass*-dominated land surface and *sand*-dominated land surface. As a result of the different thermal and hydrologic behaviour of *grass* and *sand,* the greatest deviations from the linearity occur for the latent heat-flux and the soil heat-flux.

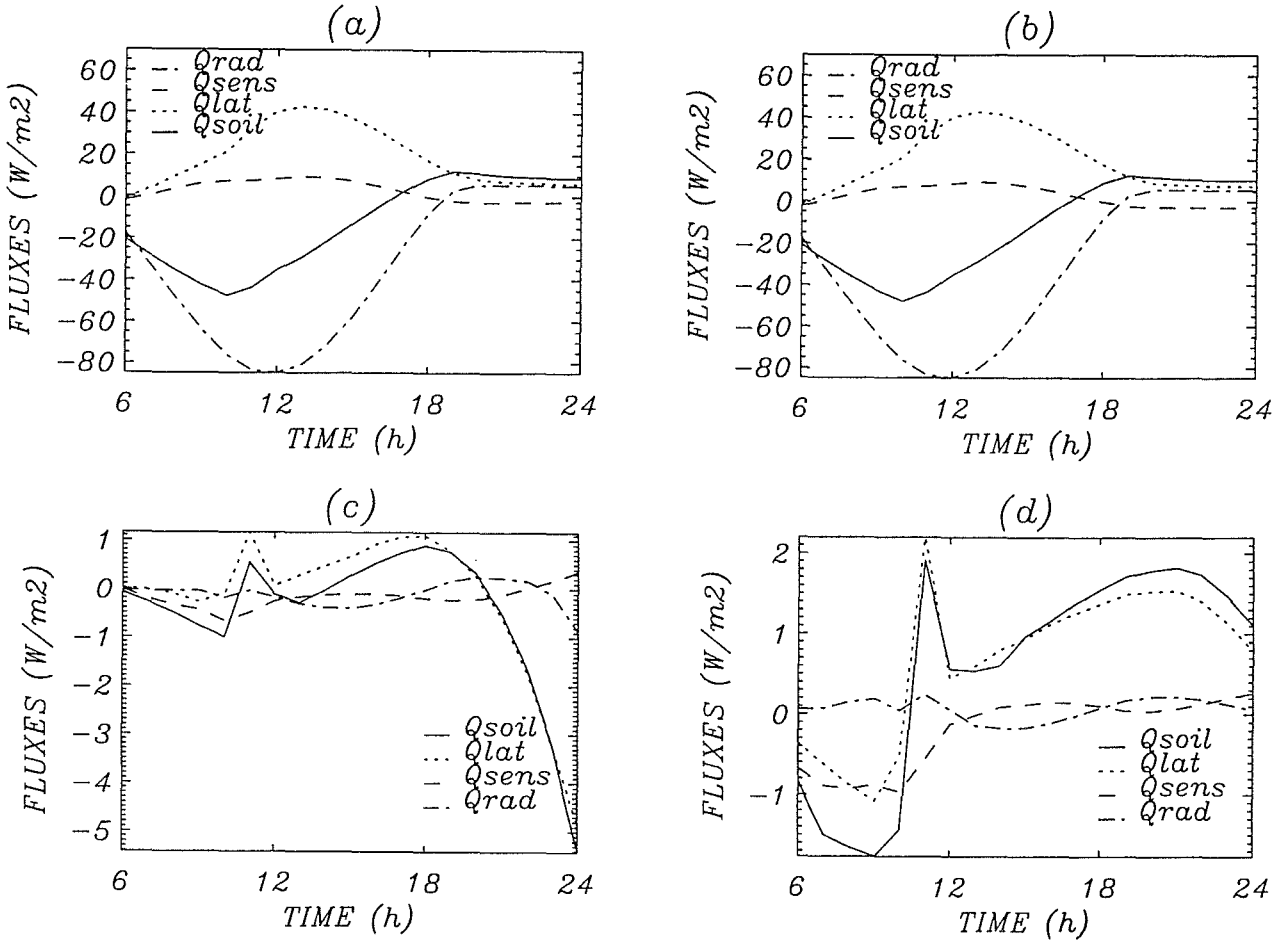

Fig. 4. Energy budgets arranged according to the degree of heterogeneity for simulations: (a) GSGC10 (b) GSGC5, (c) GSGC10-SGSC10, (d) GSGC5-SGSC5. Notice that further results of energy budget are shown in Fig. 6 under the condition of same amount of land use but different heterogeneity. All fluxes are domain averages.

4.1.1. Domain-averaged latent heat-fluxes of simulations with *grass* as the dominant land use

In the following two subsections we drop the extension GSG when addressing the simulations. When comparing all simulations in which *grass* is the dominant underlying surface, the domain- averaged latent heat-flux differs during the whole simulation time from 0800 to 2400 LT (Figs. 4 a and 4b). The maximum of the latent heat-flux occurs in all simulations at about 1300 LT with a value of 40-44 W/m². The maximum of the latent heat-flux for simulation HOMG is about 4 W/m² larger than for the most heterogeneous simulation (C5 - Fig. 4b). When comparing the least heterogeneous simulation (X25) with the most heterogeneous simulation (C5) (Tab. 2) deviations of about 2-4 W/m² less are obtained for the latter between 1000-1500 LT and deviations of about 7 W/m² less are found between 1700-2400 LT for C5 (Fig. 4b). If one looks for the degree of heterogeneity in more detail, one will usually find mostly no differences except in the juxtaposition of simulations P25 and R25. Compared to P25, simulation R25 has a decrease of 2-4 W/m² and a reduction of 4-5 W/m² in

the morning and after sunset. Furthermore, an exception is found for the juxtaposition of simulations R5 and C10 as well as for the juxtaposition of simulations C10 and C5 (Figs. 4a and 4b). Here, the latent heat-fluxes increase 1-2 W/m² for the more heterogeneous simulation.

4.1.2. Domain-averaged soil heat-fluxes of simulations with *grass* as the dominant land use

If the domain is mainly covered by *grass*, in the morning the temporal development of the behaviour of the domain-averaged soil heat-flux will hardly differ from that of the latent heat-fluxes for the simulations with the *grass*-dominated land cover. Between 0700-1300 LT we find a slight increase (1-2 W/m²) of soil heat-flux in the juxtaposition of simulations P25 and R25 as well as for simulations X2 and C5 (Fig. 4b). A more obvious difference between the domain-averaged soil heat-flux and the domain-averaged latent heat-flux occur after sunset. Generally, the increase ranges from 2-10 W/m² for the more heterogeneous surfaces (Tab. 2). For example, in comparing the domain-averaged soil heat-flux: simulations P25 and R25 have a difference of 8 W/m², simulations R25 and R5 differ about 4 W/m², and for simulations X25 and C5 (Fig. 4b) have a 10 W/m² difference. An exception is found for the comparison of the domain-averaged soil heat-fluxes of R5 to C10 as well as for the juxtaposition of C10 and C5 (Figs. 4a and 4b), where the more heterogeneous simulations (Tab. 2) have a stronger (about 1-3 W/m²) soil heat-flux than the less heterogeneous ones. A small differentiation is found for some simulations between 1900 and 2000 LT. Finally, the soil heat-flux of HOMG gets an increase of 3 W/m² towards the most heterogeneous simulation.

4.1.3. Domain-averaged latent heat-fluxes of simulations with *sand* as the dominant land use

For purposes of simplicity, we drop the extension SGS in the following two subsections when addressing the simulations. In the simulations in which the underlying surface is mostly covered by *sand* (Figs. 4c and 4d) there is obviously no linear increase of latent heat-flux or soil heat-flux from the most heterogeneous to the homogeneous, as was found for the simulations in which the underlying surface was mainly dominated by *grass* (Figs. 4a and 4b).

A slight enlargement of the latent heat-flux maximum from 40 W/m² for HOMS to 42 W/m² is found for the most heterogeneous simulation (C5). Before and after the maximum which occurs between 1200-1500 LT, we find a slight increase of 1-4 W/m² for the more heterogeneous simulations, especially for the comparison of X25 with P25 and R25 with R5. Generally, there is a reduction of latent heat-flux for *sand*-dominated land use of about 4 W/m² after sunset when comparing the least heterogeneous simulation (X25) with the most heterogeneous simulation (C5 - Fig. 4d). In juxtapozing the less heterogeneous with the next more heterogeneous simulation (Tab. 2), we do not get a linear increase as expected. Instead, an increase is investigated for the more heterogeneous simulations of 1-5 W/m² for simulations X25 and P25, R25 and R5 and for simulations R5 and C10 (Fig. 4c), as well as for simulations R5 and C5 (Fig. 4d). A reduction of 1-5 W/m² for the more heterogeneous simulation is observed for simulations P25 and R25 as well as for simulations C10 and C5 (Figs. 4c and 4d). A comparison of the results (obtained by the simulation assuming those strips perpendicular and parallel to the geostrophic wind) showed that the latent heat-flux in the case of strips parallel to the geostrophic wind is about 4-6 W/m² higher than the latent heat-flux of strips perpendicular to the geostrophic wind.

4.1.4. Domain-averaged soil heat-fluxes of simulations with *sand* as the dominant land use

Like the domain-averaged soil heat-fluxes, obtained from the simulations in which the underlying surface is dominated by *grass* (Figs. 4a and 4b), the domain-averaged soil heat-flux shows a different temporal behaviour and sensitivity than the domain-averaged latent heat-flux. We find no general tendency between the results of the homogeneous and the most heterogeneous simulations and the dependency of the soil heat-flux on increasing heterogeneity (Tab. 2). Only in the morning the domain-averaged soil heat-flux increases slightly for 1-3 W/m² between 1000-1400 LT in the case of the more heterogeneous surfaces when comparing simulations P25 with R25, simulations R5 with C10 as well as simulations C10 with C5 (Figs. 4c and 4d). On the other hand, by comparing simulations R25 with R5, the domain-averaged soil heat-flux decreases for about 1-3 W/m² for the more heterogeneous cases (Tab. 2). After 1800 LT, the domain-averaged soil heat-flux rises by 4 W/m² when comparing HOMS with C5. By juxtapozing the results of the heterogeneous with the next heterogeneous simulations (Tab. 2), we observe a decrease for simulations X25 and P25 (1-8 W/m²), R25 and R5 (1-3 W/m²), R5 and C10 (1-3 W/m²), while there is an enlargement of 1-8 W/m² for the pairs P5 and R5, as well as for the pairs C10 and C5 (Figs. 4c and 4d).

4.2. Net radiation-flux, soil heat-flux, sensible heat-flux and latent heat-flux in simulations with the same amount of land use but different heterogeneity

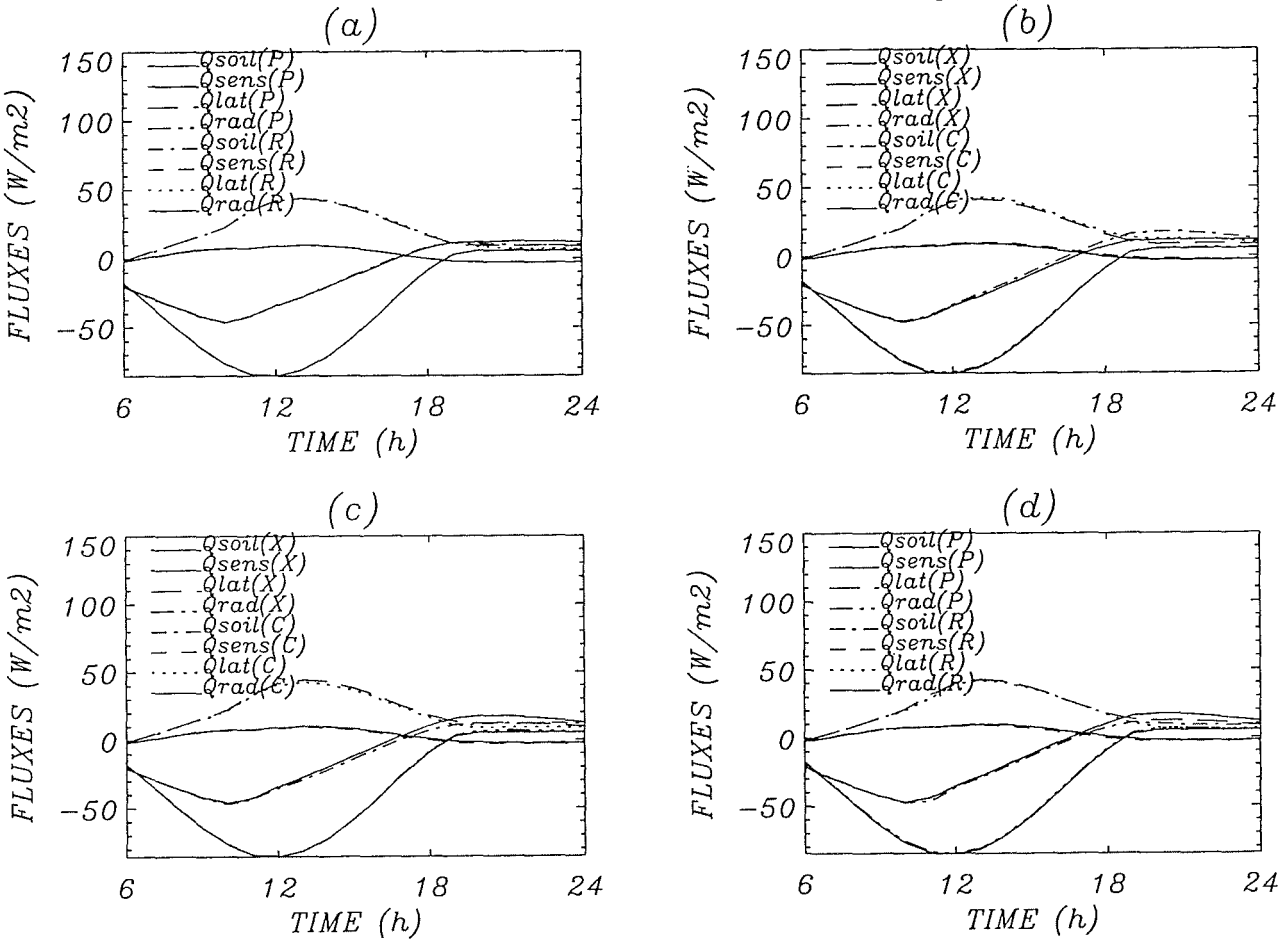

Fig. 5. Comparison of domain averaged energy budget of simulations with the same amount of *grass* and *sand* but different heterogeneity for (a) 66,7 % (GSGR25/P25) (b) 55,6% (GSGC25/X25) (c) 44,4% (SGSC25/X25) and (d) 33,3% (SGSR25/P25) *grass*.

In the previous section, we discusse the energy budget of simulations with varying amounts of *sand* and *grass* land use (Tab. 1) and different heterogeneity (Tab. 2). In this section we will

focus on the energy budget of simulations with the same amount of *grass* or *sand* but different heterogeneity. Figure 5 illustrates the dependency of the energy budget on heterogeneity.

The impact of heterogeneity on the energy budget is investigated by the juxtaposition of the simulations xxxP5 and xxxR5 (while xxx stands for GSG and SGS, respectively), where the 5 km strips are orientated parallel and perpendicular to the wind, respectively. The results show that a patch size of 5 x 5 km^2 is too small for developing a different energy budget. This coincides well with Shuttleworth's hypothesis (1991).

In simulations with a strip length of 25 km (xxxR25/P25), the sensible heat-flux and the soil heat-flux start to increase about 1-2 W/m^2 after 1200 LT, while the greatest differences for the soil heat-flux achieve up to 10 W/m^2 LT after sunset (Fig. 5a and 5d). The differences between xxxX25 and xxxC25 increase about 2-3 W/m^2 before sunset and up to 6 W/m^2 afterwards (Figs. 5b and 5c).

4.3. Domain-averages of the latent heat-fluxes obtained by the simulations with homogeneous underlying surface compared to those without, i.e. heterogeneous

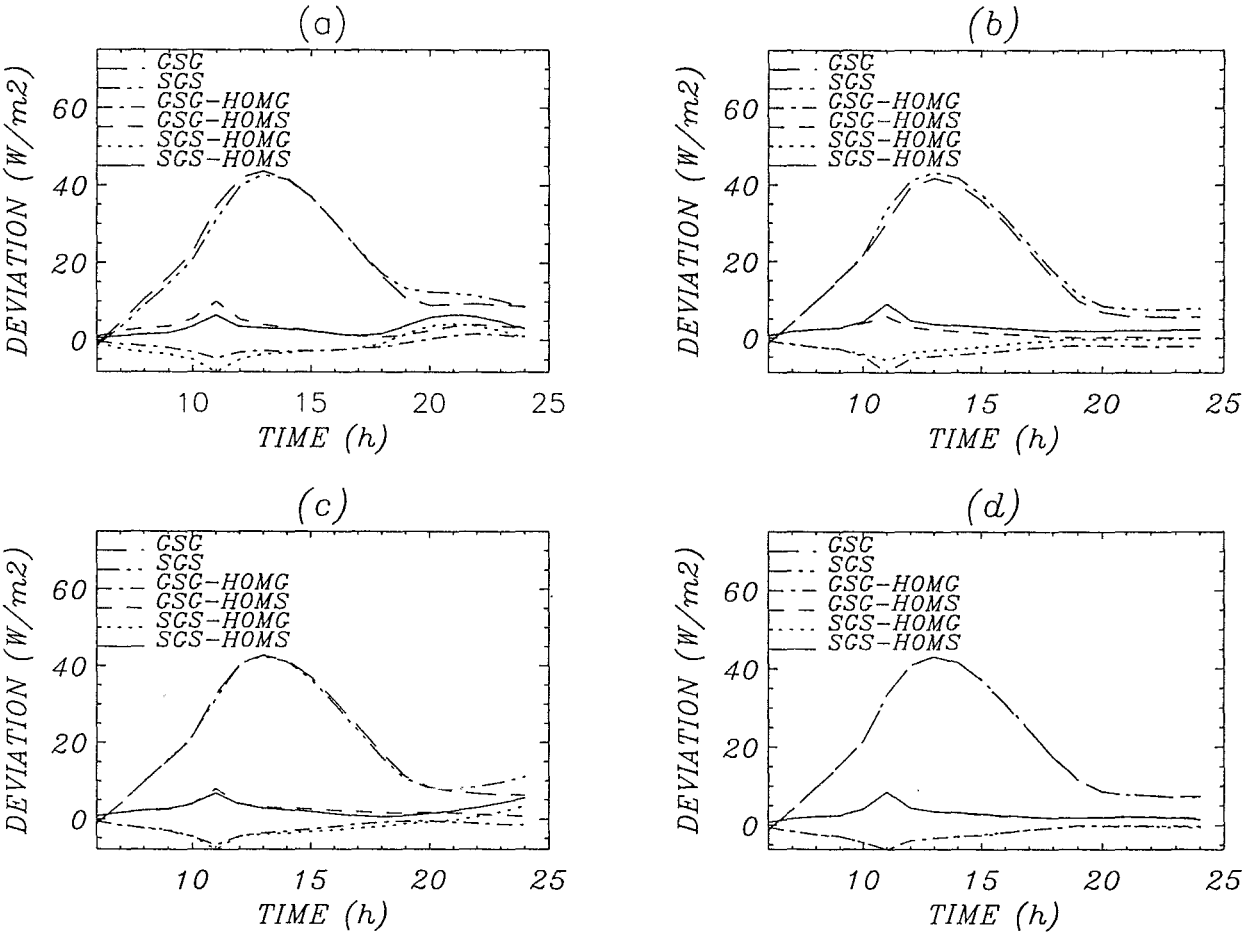

Fig. 6. Difference of domain averaged latent heat-flux for (a) xxxP25-HOMx representing the 3π-sinus curve (b) xxxR5-HOMx describing the π-sinus curve and (c) xxxC10-HOMx expressing the $5/2\pi$-sinus and (d) xxxP5-HOMx. Note that xxx stands either for GSG or SGS and x represents *sand* or *grass*, respectively.

The domain averages of the simulations with heterogeneous land use (called HET hereafter) were subtracted from the results of the simulations with homogeneous *grass* as well as with homogeneous *sand* (Fig. 6). In the following description xxx stands for all possibilities: either all heterogeneous land use (GSG or SGS) or all patch-style contributions (R25, P5, etc.).

Notice HETxxx means all domain-averaged heat-fluxes of all heterogeneous simulations, while HETG = GSGxxx-HOMS = SGSxxx - HOMS and HETS = GSGxxx - HOMG = SGSxxx - HOMG. Be aware that the differences in chapter 4.4 are fractional-weighted latent heat-fluxes (Eq. 1), while here the contribution of the fractions of equal land use are compared.

The latent heat-flux is the most sensitive component of the energy budget with respect to changes in heterogeneity. Therefore, we will limit the discussion to this aspect. Generally, the differential HETxxx-HOMG of the latent heat-flux decreases till 1100 LT, followed by an increase till 1900 LT. After subtracting the latent heat-flux of HOMG from those of SGSxxx and GSGxxx (which leads to HETS), the differences provide a minimum at 1100 LT in all simulations ranging from -4 till -11 W/m² and a maximum in the afternoon and evening (1900-2400 LT) of -1 till 4 W/m² in some simulations. Two different patterns of behaviour were obtained after sunset for the results of HETS:

1. The first is a slight decrease with a tendency to stagnation between 1900-2400 LT in simulations with smaller patches like xxxC10-HOMG (Fig. 6c), xxxC5-HOMG, xxxP5-HOMG (Fig. 6d), xxxR25-HOMG .
2. The second is a maximum at 2100 LT and a decrease afterwards in simulations with coarser patches like xxxP25-HOMG (Fig. 6a), xxxX25-HOMG, xxxC25-HOMG.

Notice the same subtractions are done for HOMS and SGSxxx/GSGxxx (which leads to HETG). There the simulations again behave after special shapes (Tab. 3).

As pointed out before, assuming a linear behaviour between the increase/decrease in the latent heat-flux and the increase in the fractionally coverage of the model domain by *grass/sand* (under conditions without rain or dew), the greatest domain-averaged latent heat-flux is expected for homogeneous *grass* followed by the heterogeneous *grass*-dominated conditions, and finally by the heterogeneous *sand*-dominated conditions. However, some exceptions to the above assumption were observed. This is mainly visible when the domain-averaged latent heat-flux, provided by the simulation with the homogeneously *sand*-covered surface (HOMS), is subtracted from that provided by the simulations with the heterogeneous surfaces. The resulting values of latent heat-flux of the *grass*-covered fraction (SGSxxx-HOMS = HETG or GSGxxx-HOMS = HETG) become positive. On the other hand, the latent heat-fluxes provided by the simulation with homogeneous *grass* coverage, minus those with the heterogeneous coverage simulations (GSGxxx-HOMG = HETS or SGSxxx-HOMG = HETS), receive latent heat-fluxes which are directed to the ground. This deviation of the domain-averaged latent heat-fluxes from the linear assumption is as followes:

- xxxC25: 1200-2000 LT HOMG>SGSxxx>GSGxxx
  2000-2400 LT SGSxxx>GSGxxx>HOMG
- xxxP25 (Fig. 6a): 1700-2400 LT SGSxxx>GSGxxx>HOMG
- SGSC10 (Fig. 6c): 2100-2400 LT SGSxxx>HOMG>GSGxxx
- xxxX25: 0000-1900 LT HOMG>GSGxxx>HOMS
- xxxR5 (Fig. 6b): 0900-2400 LT HOMG>SGSxxx>GSGxxx

These effects only occur for the latent heat-fluxes resulting *grass* (HETxxx-HOMS), because the latent heat-flux of homogeneous *sand* does never exceed that of the simulations with a heterogeneous land cover. Only in simulations GSGC25 (0000-1200 LT), GSGP25 (1700-2400 LT), GSGC10 (2000-2400 LT) and GSGR5 (0900-2400 LT) the heterogeneous *sand* dominated land use exceeds the latent heat-flux of the heterogeneous *grass* dominated land use. As mentioned before, all these results are obvious in the energy budget in Fig. 4 as well.

There is no correlation between the onset of the irregularity and the amount of *sand* or *grass*. It seems that the starting depends on the arrangment of patches (Tab. 2), e.g., the starting point for xxxC25 is later than for xxxP25.

Finally, in the simulations assuming an underlying surface of 5 km wide strips parallel to the geostrophic wind, we find no differences between the latent heat-flux of SGSP5-HOMG (which represents the contribution of the *sand*-covered patches to the domain-

averaged flux) and GSGP5-HOMG (that also represents the contribution of the *sand* covered patches to the domain averaged flux !). Notice that both results from the subtraction lead to *sand* (HETS) but the amount of *sand* is different while the latent heat-flux is equal (Fig. 6d).

For the differentials of the results of HOMS minus those of all heterogeneous simulations (which leads to HETG) an opposite behaviour than that of the differences of HETS is expected. Nevertheless, this is only confirmed by the latent heat-flux of xxxR25-HOMS and xxxR5-HOMS (Figs. 6a and 6b). While the latter converge against each other for the whole simulation time, all other simulations converge against one another till 1700 LT (Fig. 6). Afterwards the temporal evolution of the domain-averaged fluxes is parallel to each other (from 1700-2400 LT). The maximum of the differentials of the latent heat-flux is found at 1100 LT with a value of about 6-9W/m².

Curve shape	**Time of the first maximum (value)**	**Time of the second maximum (value)**	**Time of the first minimum (value)**	**Simulations representing HETG**
3π sinus	1100 LT (6-10 W/m²)	21/2200 LT (3-7 W/m²)	1800 LT (0.5-2 W/m²)	xxxC25-HOMS xxxP25-HOMS xxxX25-HOMS
π sinus	1100 LT (6-11 W/m²)			xxxR25-HOMS GSGC10-HOMS GSGC5-HOMS xxxP5-HOMS xxxR5-HOMS
$5/2\pi$ sinus	1100 LT (6-10 W/m²)	2400 LT (5 W/m²)	1800 LT (1-2 W/m²)	SGSC10-HOMS SGSC5-HOMS

Tab. 3. Classification of the effects of heterogeneity according to the temporal behaviour of the differences between the simulations assuming homogeneous land cover, HOMx, and those assuming heterogeneous land cover, namely HETxxx. Note that xxx stands for the patch style contribution, respectively.

We distinguishe between three different patterns of behaviour of the curve of the differentials, namely, a π-sinus, a 3π-sinus, and a $5/2\pi$-sinus curve-like behaviour (Tab. 3). Notice that for the simulations with a curve like a 3π-sinus the greatest deviations are found for xxxX25-HOMS. The simulations refer to as xxxC25-HOMS and xxxP25-HOMS are similar in their behaviour with a greater difference of xxxP25-HOMS and an irregular behaviour after sunset. The greatest deviations from linearity as well as irregularity (which were discussed already in the context with xxxR25-HOMS) are found in the simulations providing a π-sinus curve of the differences.

An exception to the behaviour after 1900 LT is found in simulations xxxC10 (Fig. 6c), for which SGSC10-HOMS and SGSC10-HOMG increase. For the latter differences, two maxima of 5 and 3 W/m² occur at 2400 LT. The differentials GSGC10-HOMG and GSGC10-HOMS decrease after a maximum at 2000 LT till 2400 LT.

4.4. Comparison of fractionally weighted heterogeneous to fractionally weighted homogeneous simulation of latent heat-flux

The domain averages of fluxes obtained by the simulations with heterogeneous land use were subtracted from the fractionally weighted domain averages of the simulations with a homogeneous coverage by *sand* or *grass*, respectively.

By comparing the fractionally weighted latent heat-flux of the 'homogeneous' with that of the 'heterogeneous' simulation (by using Eq. 1), we get a closer look at how heterogeneity

effects the energy budget. The magnitude of the differences varies over a wide range from simulation to simulation, but the greatest differences are found in the evening after sunset.

To evaluate the temporal development and the magnitude of the non-linear behaviour of the latent heat-flux due to heterogeneity of land use, the differential of (1-α)HETS was compared to (1-α)HOMS and the differential of αHETG was compared to αHOMG, respectively (Fig. 7).

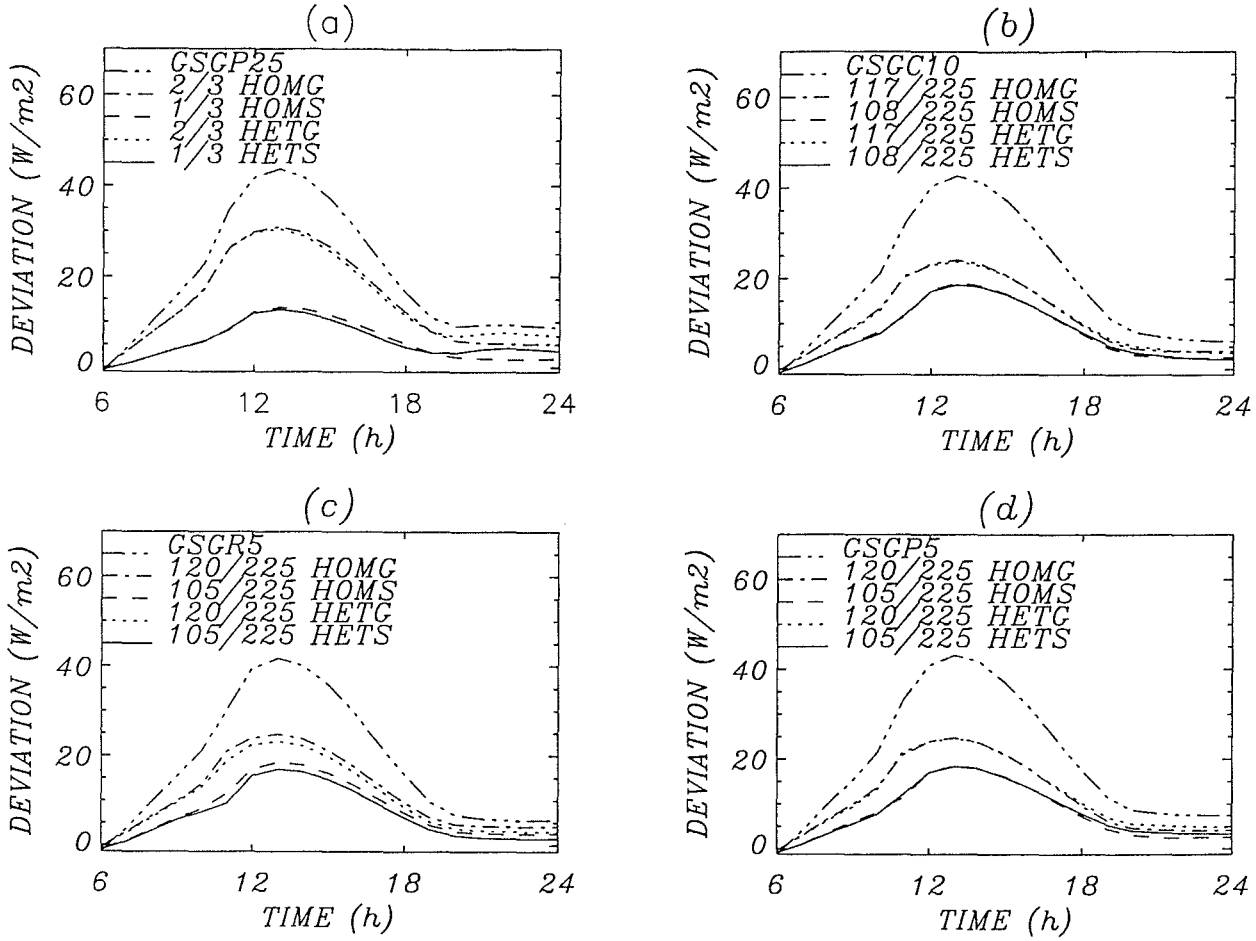

Fig. 7. Fractional weighted latent heat-flux representing the differences of heterogeneous simulations to homogeneous simulations of *grass* for (a) GSGP25, (b) GSGC10, (c) GSGR5 and (d) GSGP5. All fluxes are domain averages.

Time of greatest differences of (1-α)HETS and αHETG	**Simulation with the heterogeneous land cover**
1100	SGSR25 SGSR5
1300	GSGR25
after sunset	xxxC25 xxxP25 GSGC5 xxxX25 xxxP5
1300 and 2100	GSGR5

Tab. 4. Grouping of the simulations according to the magnitude of β. Here, xxx stands for GSG and SGS, respectively. Parameters are used as explained for Eq. 1.

Since the differences on the left-hand side of Eq. 1 are similar for *sand* and *grass* in magnitude and their temporal behaviour, the following comments are valid for both. We create four groups of simulations with an identical onset of great differences and, hence, a β which is not equal to 1 (Tab. 4).

Furthermore, we focuse on the magnitude of the comparison between the latent heat-flux of fractionally weighted homogeneous land use and fractionally weighted homogeneous when subtracting from fractionally weighted heterogeneous land use. We get a detailed view compared to Tab. 4 where the latent heat-flux is higher, either in the heterogeneous or in the homogeneous fraction according to Eq. 1. In doing so, we found the five kinds of similar behaviour as listed in Tab. 5.

In Tab. 5, the role of heterogeneity on the energy budget is obviously seen with a variation of higher and lower latent heat-fluxes for heterogeneous land use compared to homogeneous land use. Without consideration of the heterogeneity of land use, the value of latent heat-flux of a 'homogeneous (dominant) land use' will be mostly calculated too high, while after sunset it will be calculated too low.

No		Simulation name x=*sand* and *grass*	Time of difference	Magnitude of difference
1.	$(1-\alpha)$ HETS < $(1-\alpha)$ HOMS α HETG < α HOMG	GSGC25 GSGP25	1100-1900 LT	1-3 W/m²
	$(1-\alpha)$ HETS > $(1-\alpha)$ HOMS α HETG > α HOMG	SGSC5 GSGC5 GSGX25	1900-2400 LT	1-5 W/m²
2.	$(1-\alpha)$ HETS > $(1-\alpha)$ HOMS α HETG > α HOMG	SGSC25 SGSP25 SGSX25 SGSR5	1000-1500 LT 1800-2400 LT	1-3 W/m² 1-8 W/m²
3.	$(1-\alpha)$ HETS < $(1-\alpha)$ HOMS α HETG < α HOMG	SGSR5	1000-1200 LT	1 W/m²
		GSGR25	1200-1400 LT	1 W/m²
		SGSC5 GSGR5	1000-2400 LT	1-3 W/m²
4.	$(1-\alpha)$ HETS > $(1-\alpha)$ HOMS α HETG > α HOMG	GSGP5	1800-2400 LT	1-2 W/m²
5.	$(1-\alpha)$ HETS > $(1-\alpha)$ HOMS	GSGC10	1800-2200 LT	1 W/m²
	$(1-\alpha)$ HETS < $(1-\alpha)$ HOMS		1200-1400 LT 2200-2400 LT	1 W/m²

Tab. 5. Grouping of the simulations according to their temporal behaviour of non-linearity with respect to Eq. 1. Here, xxx stands for GSG and SGS. Parameters are used as explained for Eq. 1.

The maximum of latent heat-flux of the fractionally weighted homogeneous and heterogeneous simulations is achieved at 1300 LT (Fig. 7). The value of the greatest latent heat-flux of fractionally weighted homogeneous or heterogeneous land-use *grass* ranges between 16 and 31 W/m² depending on the amount of *grass*. While the maximum of fractionally weighted homogeneous or heterogeneous land-use *sand* strays from 12 to 27 W/m² correlating with the amount of *sand*. Despite some exceptions (Tab. 5, No.2) the fractionally weighted homogeneous maximum of latent heat-flux is usually a little higher (1-2 W/m²) than the fractionally weighted heterogeneous maximum at 1300 LT. Generally, during daytime, the latent heat-flux of the fractionally weighted homogeneous simulation has a slightly larger amount than the fractionally weighted heterogeneous simulation and has a slightly smaller amount after sunset.

The minimum of the latent heat-flux of the fractionally weighted heterogeneous and homogeneous simulations appears after sunset but in different shapes (Fig. 7): First, the minimum of (1-α)HETS and αHETG is located at 2400 LT when in Eq. 1 HETx stands for GSGR25, SGSC25, SGSP25 or SGSR25, respectively. Furthermore, the latent heat-flux shows no changes after 2100 LT or the minimum occurs at 2100 LT followed by an increase afterwards, e.g. in GSGR5, GSGC10 and GSGP5. The last shape builds up two minima one at 2000 LT and one at 2400 LT. The latter will appear mainly if, in the heterogeneous simulation, the amount of *grass* and *sand* is nearly the same (45-55 %).

Finally, large deviations in the fractionally weighted heterogeneous simulations compared to the fractionally weighted homogeneous simulations may occur if the heterogeneous simulations are xxxC25, xxxR5 and xxxP25, while small or negligible deviations are found for xxxR25, xxxC10, xxxP5, xxxC5 and xxxR5.

4.5. Grid-point-by-grid-point differences of latent heat-flux

In a grid-point-by-grid-point manner, the results of HOMG are alternatively subtracted from those of all heterogeneous simulations at 1200 LT. It has to be expected that the greatest differences occur at the boundary between the patches of *sand* and *grass* land use. The latent heat-flux for HOMS is about 36 W/m² and for HOMG has a value of 44 W/m² at 1200 LT. Furthermore, we expect values close to ground zero if the land use is the same (in this case *grass*), and positive values (around 8 W/m²) if the patches are covered differently (in this case *sand*), because a *grass*-covered surface usually provides greater latent heat-fluxes than a sandy surface under the same micrometerological conditions.

As pointed out already, the results substantiate that the differences do not behave linearly to the amount of *grass* or *sand*. The size and the arrangement of the *grass* and *sand* have a great impact on the horizontal distribution of the latent heat-flux. The distributions of the differences in the latent heat-flux show no interactions between the neighbouring *sand* and *grass* patches in simulations with a *grass/sand* patch size of 5 km and in the simulations with patches arranged parallel to the geostrophic wind like HOMG-xxxC5, HOMG-xxxR5, HOMG-xxxP5 and HOMG-GSGP25. This agrees entirely with Shuttleworth's (1991) hypothesis that a 'disorganised' land surface-cover (with a length < 10 km) has not a clearly proved influence on the energy budget.

In simulation HOMG-GSGP25, no effect of heterogeneity on the latent heat-flux is found at the interface between *sand* and *grass* patches. This missing effect could be explained as a tunnel-like flow with smooth *sand* in the middle surrounded by the high and rough *grass*. On the other hand for the differential of HOMG-SGSP25, appreciable effects were detected in the northern *sand* patch with higher latent heat-flux of approximatly 5 W/m² in SGSP25 than in HOMG. This can be explained by the flow from the higher and rougher *grass* patches towards the smoother *sand*, which leads to an acceleration of the flow and, hence, increased latent heat-flux.

For the distributions of the latent heat-flux small differences in xxxC10-HOMG are obtained for the *sand* patches and no differences are inquired for the *grass* patches. This might be partly an 'organised' and random influence.

Greater interactions between the neighbouring *sand* and *grass* patches are found in the distributions of the differentials HOMG-xxxX25, HOMG-xxxC25 and HOMG-xxxR25, respectively (Fig. 8). In the simulation GSGC25 (Fig. 8a), the interaction mainly occurs at the middle strip and the east strip. For the most part there is a jump in the latent heat-flux between -3 and 12 W/m² directly at the interface between *grass* and *sand,* and a decrease from *sand* to the *grass* patches, respectively. This means an increase of the latent heat-flux for the northern and southern *sand* patches and a decrease of the eastern and western *sand* patches as compared to the case of a homogeneously *grass*-covered domain. In the heterogeneous case, the latent heat-flux of the *grass* patches is greater at the edges and smaller in the middle, compared to the homogeneous latent heat-flux of *grass*.

(a)

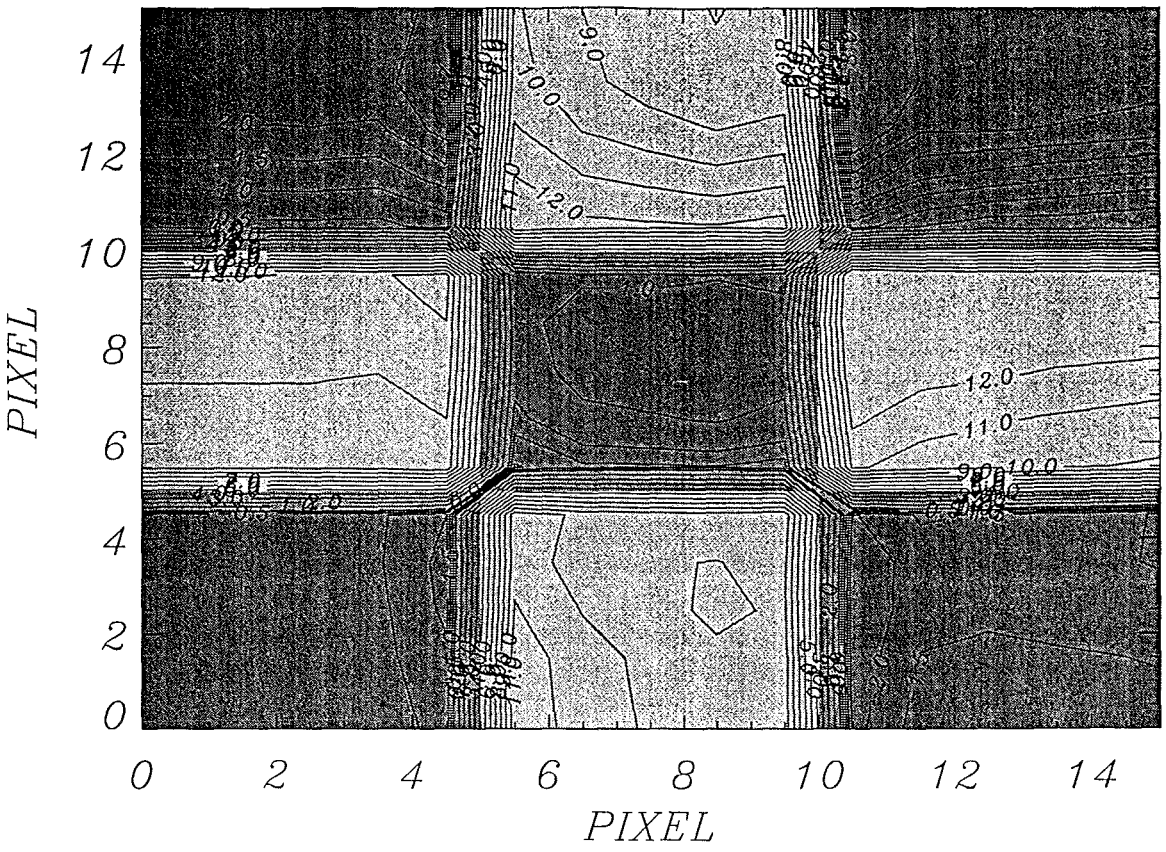
PIXEL
0
2
4
6
8
10
12
14
PIXEL
12.0
11.0
10.0

(b)

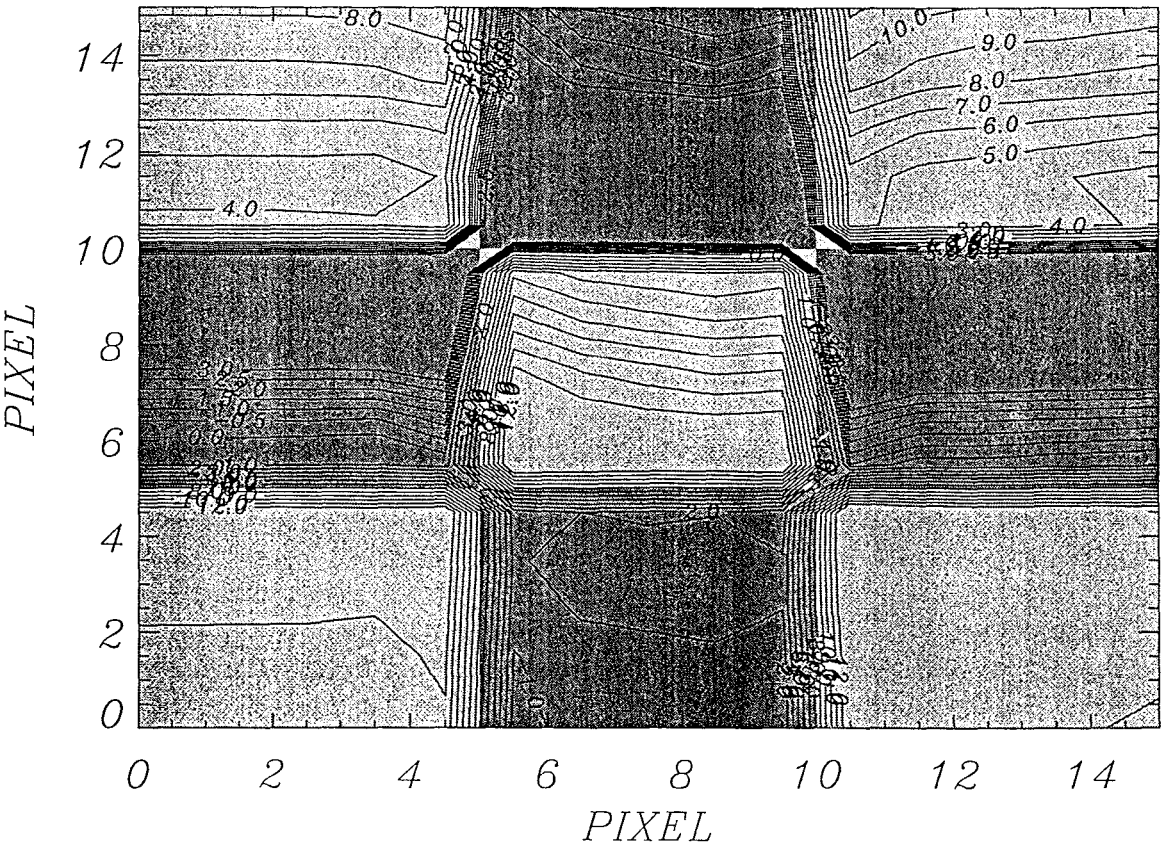
PIXEL
0
2
4
6
8
10
12
14
PIXEL
8.0
10.0
9.0
8.0
7.0
6.0
5.0
4.0

(c)

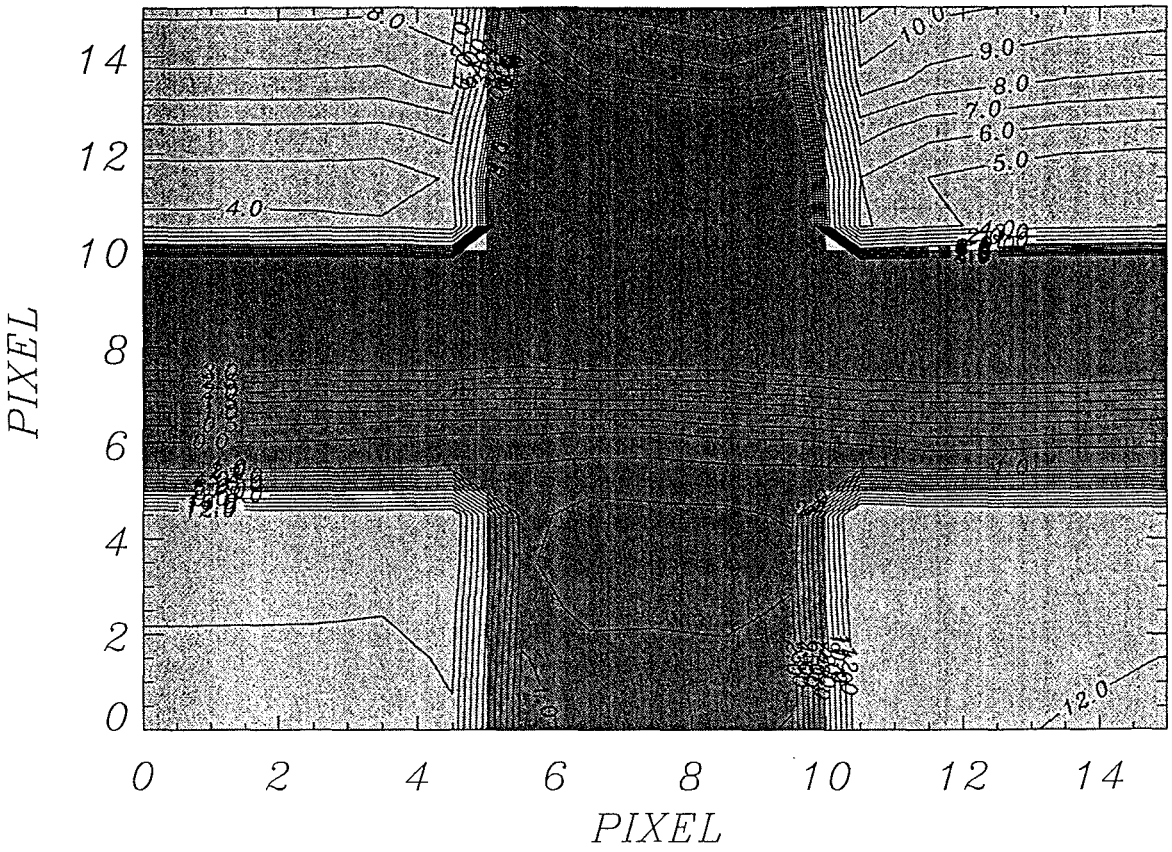
PIXEL
0
2
4
6
8
10
12
14
PIXEL
0
2
4
6
8
10
12
14
8.0
9.0
10.0
5.0
6.0
7.0
4.0
12.0

(d)

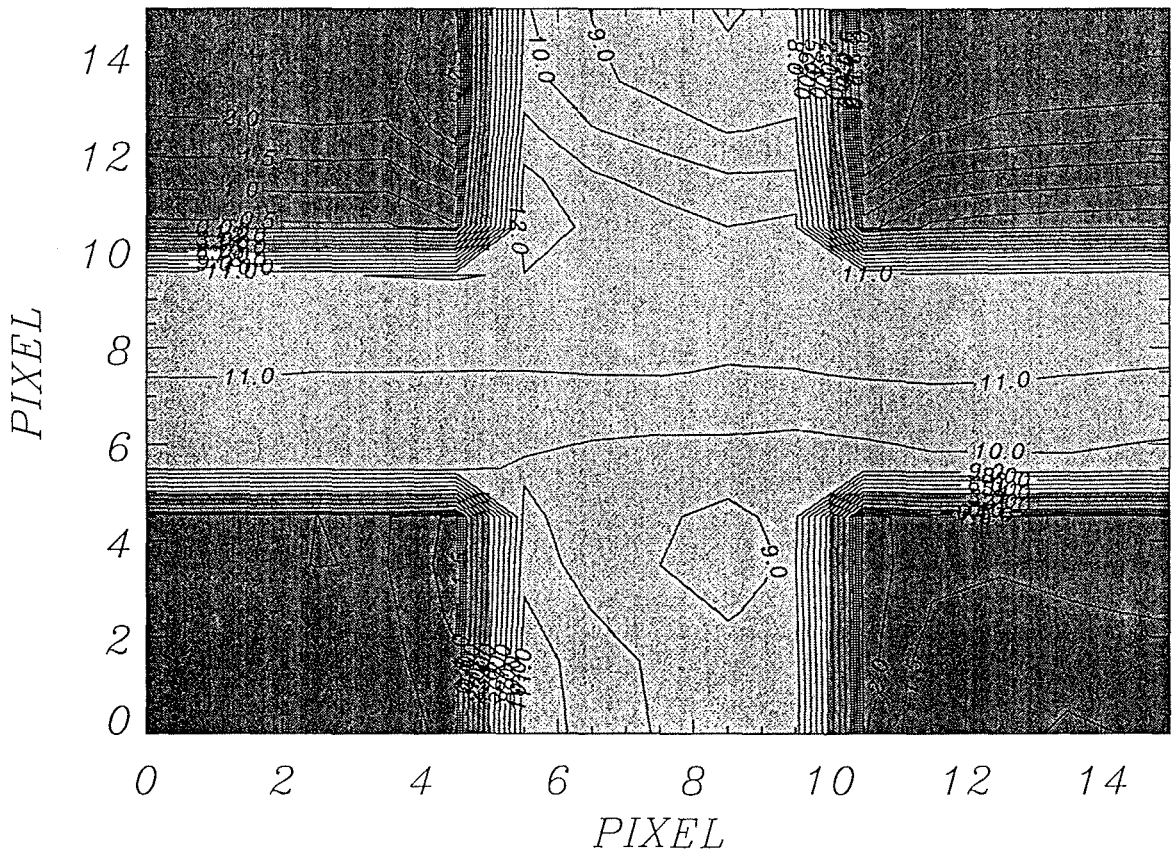
PIXEL
0
2
4
6
8
10
12
14
PIXEL
0
2
4
6
8
10
12
14
10.0
9.0
11.0
11.0
11.0
10.0
9.0

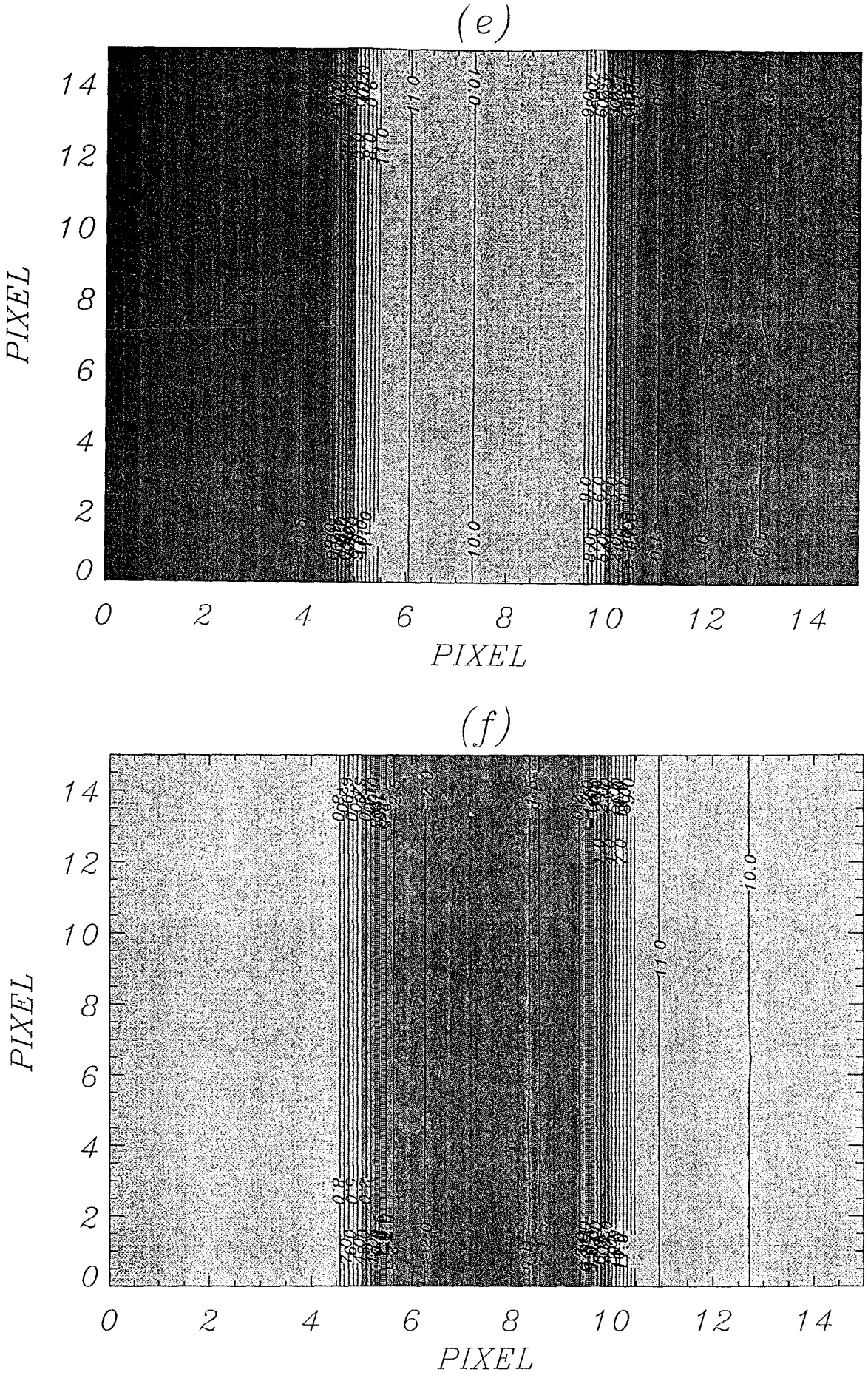

Fig. 8. Two-dimensional sections of latent heat-flux representing the difference of heterogeneous *grass* dominated simulations and HOMG and (a) GSGC25 (b) SGSC25 (c) GSGX25 (d) SGSX25 (e) GSGR25 (f) SGSR25 at 1200 LT. Grey patches indicate *grass* and light grey patches indicate *sand*, respectively.

In simulation refer to as SGSC25 (Fig. 8b), the latent heat-flux over *grass* patches are higher in the northeastern and the western part of the domain than in the simulation with a homogeneous *grass*-covered surface. The opposite is true for the southern part of the domain. In the northern *sand* patches and partial in the *sand* patch in the middle of the domain, the latent heat-flux (provided by the simulation with the heterogeneous surface) exceeds that of the simulation with a homogeneously covered *grass* surface. This indicates interactions in the northern part.

Similar differences result from the simulation called GSGX25 and SGSX25 (Fig. 8c and 8d). In simulation SGSX25 the latent heat-flux differs from those of HOMG in the northern and southern *sand* patches. No differences are found at the *grass* patches in the corners and between kilometres 5 to 10 in an east-west direction of the north-south-strip, where the wind flows without hitting obstacles.

Subtracting HOMG from GSGX25, we observed no differences in the southern part but strong interactions between neighbouring *sand* and *grass* patches in the northern part. These effects are visible till kilometre 8 in the south. Herein, the latent heat-flux of *sand* increases due to interaction with the adjacent *grass* patches.

5. Summary and Conclusions

First of all, we investigated how the degree of heterogeneity of a landscape can influence the energy and water fluxes. Although a difference of 2-4 W/m² in the morning and 2-7 W/m² in the afternoon, between the fluxes for a homogeneous and a heterogeneous surface, is very small and far beyond the accuracy of any measurements, the impact of heterogeneity on the latent heat-flux cannot be neglected. Even though the difference is just some W/m² per day, it has to be considered that a difference of 1 W/(m²•d) means an enlarged evapotranspiration of 12.6 mm/a. If we focus on the latent heat-flux of *sand* with an amount of 39.5 W/m² at 1300 LT on a day with a calm wind and a cloudy atmosphere in spring, a deviation of 2 to 8 W/m² means a difference of 5 to 20 % for *sand*. For the latent heat-flux of *grass*, this results in a difference of 4 % for 2 W/m² and 17 % for 8 W/m². Hence, the results indicate that changes in land use or simple heterogeneity do have a strong impact on the energy and water fluxes.

Nevertheless, the comparison of simulations with the same amount of land use and varying patch arrangements shows hardly any differences between simulations with a patch size of 5 km (cf. Fig. 7d). For simulations with a patch size of 25 km, however, the dependence of latent heat-flux on heterogeneity starts at 1200 LT and increases with time (Fig. 6). If we focus on simulations with same patch arrangements and varying amounts of land use (Fig. 5), the latent heat-flux approaches the value of the simulation with the homogeneous land use, that means, e.g., the more *grass* in the domain, the greater the latent heat-flux. Generally speaking, the maximum of the latent heat-flux decreases with increasing heterogeneity and increasing coverage by *grass*, except for the simulations xxxC25 and xxxP5. Nevertheless, this behaviour is not linear (cf. Fig. 3). The greatest deviations from the linearity are found around 1300 LT and after sunset.

The enlargement of latent heat-flux with increasing heterogeneity is at the expense of the sensible heat-fluxes and soil heat-fluxes. Therefore, with some exceptions, the soil heat-flux and the latent heat-flux decrease by increasing heterogeneity, while the sensible heat-flux increases. Note that these exceptions can result from the arrangement of simulations we used to classify the heterogeneity in Tab. 2.

When comparing the results from simulations with different heterogeneity, the simulations with a patch length < 10 km are found to have no influence on the daily or annual energy budget, i.e., patches with a length < 10 km give no apparent 'organised' response to the atmospheric boundary layer. The latent heat-fluxes of simulations with a larger patch size than 10 km clearly response to heterogeneity. This is manifested by the comparison of the latent heat-fluxes provided by simulations with same amount of land use but different heterogeneity.

For instance, the energy budget of xxxR25 and xxxP25 differs less than that of xxxX25. The same is true for the distributions of the differences xxxP5-HOMG and xxxC10-HOMG.

Based on these findings, we may conclude that changes in land use or simple heterogeneity may have a strong impact on the local water and energy fluxes and, therefore, on the variables of state and local meteorological processes taking place.

6. Acknowledgments

This study was financially supported by the DFG under contracts Mo770/1-1 and Mo770/1-2 and by the BMBF under contracts 521-4007-07 VWK 01 and LT2.D.2.

7. References

Anthes, R.A., 1984. Enhancement of convective precipitation by mesoscale variations in vegetative covering in semiarid regions. *J. Clim. and Appl. Met.* **23**, 541-554.

Avissar, R., R.A. Pielke, 1989. A parameterization of heterogeneous land surface for atmospheric numerical models and its impact on regional meteorology. *Mon. Wea. Rev.* **117**, 2113-2136.

Deardorff, J.W., 1978. Efficient prediction of ground surface temperature and moisture, with inclusion of a layer of vegetation. *J. Geophys. Res.* **84C**, 1889-1903.

Eppel, D.P., H. Kapitza, M. Claussen, D. Jacob, W. Koch, L. Levkov, H.-T. Mengelkamp, N. Werrmann, 1995. The non-hydrostatic mesoscale model GESIMA. Part II: Parameterizations and applications. *Contrib. Atmos. Phys.* **68**, 15-41.

Kapitza, H., D.P. Eppel, 1992. The non-hydrostatic mesoscale model GESIMA. Part I: Dynamical equations and tests. *Contr. Phys. Atmos.* **65**, 129-146.

Kramm, G., R. Dlugi, D.J. Dollard, T. Foken, N. Mölders, H. Müller, W. Seiler, H. Sievering, 1995. On the dry deposition of ozone and reactive nitrogen compounds. *Atmos. Environ.* **29**, 3209-3231.

Mahrt, L., J. Sun, D. Vickers, J.I. MacPherson, J.R. Pederson, 1994. Ozone fluxes over patchy cultivated surface. *J. Geophys. Res.* **100D**, 23125-23131.

Mölders, N., A. Raabe, 1996. Numerical investigations on the influence of subgrid-scale surface heterogeneity on evapotranspiration and cloud processes. *J. Appl. Meteor.* **35**, 782-795.

Mölders, N., G. Kramm, M. Laube, A. Raabe, 1997. On the influence of bulk parameterization schemes of cloud relevant microphysics on the predicted water cycle relevant quantities - a case study. *Meteorol. Zeischr.* **6**, 21-32.

O'Neal, 1996. Interactions between land cover and convective cloud cover over Midwestern North America detected from GOES satellite data. *Int. J. Remote Sensing* **17**, 1149-1181.

Shen, S., M.Y. Leclerc, 1994. Large eddy simulation of small-scale surface effects on the convective boundary layer. *Atmosphere-Ocean* **32**, 717-731.

Shuttleworth, W.J., 1988. Macrohydrology - the new challenge for process hydrology. *J. Hydrology* **100**, 31-56.

Shuttleworth, W.J., 1991. Insight from large-scale observational studies on land/atmosphere interactions. *Surveys in Geophysics* **12**, 3-30.

Address of the authors:

LIM - Institut für Meteorologie
Universität Leipzig
Stephanstraße 3
04103 Leipzig
Germany